tvst

DOI: 10.1167/tvst.5.3.11

Article

Localized RPE Removal with a Novel Instrument Aided by Viscoelastics in Rabbits

Fabian Thieltges[1], Zengping Liu[1,*], Ralf Brinken[1], Norbert Braun[2], Warapat Wongsawad[3], Sudawadee Somboonthanakij[3], Martina Herwig[1], Frank G. Holz[1], and Boris V. Stanzel[1,#]

[1] Department of Ophthalmology, University of Bonn, Bonn, Germany
[2] Geuder AG, Heidelberg, Germany
[3] Mettapracharak Eye Institute, Raikhing, Nakhon Pathom 73210, Thailand
[*] Present address: Zengping Liu, Department of Ophthalmology, National University of Singapore, Singapore
[#] Present address: Singapore National Eye Center, Singapore

Correspondence: Fabian Thieltges, Universitäts-Augenklinik Bonn, Ernst Abbe-Str. 2, 53127 Bonn, Germany. e-mail: fathie@uni-bonn.de
Boris V. Stanzel, Singapore National Eye Center, Surgical Retina Department, 11 Third Hospital Ave, Singapur 168751. e-mail: stanzel@uni-bonn.de

Received: 29 May 2015
Accepted: 5 April 2016
Published: 1 June 2016

Keywords: AMD, Bruch's membrane, cell-based therapy, cell replacement, hyaluronic acid, hydrogel, retina, retinal surgery, RPE transplantation, tissue engineering

Citation: Thieltges F, Liu Z, Brinken R, Braun N, Wongsawad W, Somboonthanakij S, Herwig M, Holz FG, Stanzel BV. Localized RPE removal with a novel instrument aided by viscoelastics in rabbits. Trans Vis Sci Tech. 2016;5(3):11, doi:10.1167/tvst.5.3.11

Purpose: We developed a surgical method for localized and atraumatic removal of the retinal pigment epithelium (RPE) with a novel instrument.

Methods: Bleb retinal detachments (bRD) were raised with balanced salt solution (BSS) following vitrectomy in 27 rabbits. The RPE was scraped with 3 loop variants (polypropylene [PP], 0.1 mm; PP, 0.06 mm; metal, 0.1 mm) of a custom-made instrument. Stabilization of bRDs with BSS or various concentrations (0.1%–0.5%) of hyaluronic acid (HA) was video analyzed. Perfusion-fixed samples of scraped areas and controls were studied by light and transmission electron microscopy.

Results: The bRDs were sufficiently stabilized by $\geq$0.25% HA. Using the PP 0.1 mm loop with a single forward/backward stroke, an area of ca. 2.5 $\times$ 1.5 mm was nearly devoid of RPE, yet did show occasional Bruch's membrane (BM) defects combined with choriocapillaris hemorrhages in 13% of the bRDs. A single scrape with PP 0.06 mm resulted in unsatisfactory RPE denudement, while repeated scraping maneuvers caused more BM defects and hemorrhages. The metal loop resulted in incomplete RPE removal and massive intraoperative subretinal hemorrhages. Histologically, intact photoreceptor outer segments (POS) were observed above the RPE wounds in bRDs. Controls with bRDs alone showed an intact RPE monolayer with microvilli, with few engulfed remains of POS.

Conclusions: Localized removal of RPE in HA stabilized bRD can be achieved by a PP 0.1 mm loop instrument.

Translational Relevance: Removal of degenerated RPE may aid RPE cell replacement strategies.

Introduction

Retinal pigment epithelial (RPE) transplantation has the potential to offer a curative therapy for patients suffering from retinal diseases affected with RPE dysfunction.[1] Several cell sources for RPE replacement have been investigated, including adult autologous and fetal allogeneic RPE, embryonic, and induced pluripotent stem cell-derived RPE, neural stem cells, or mesenchymal stromal cells.[2–7]

There are two main techniques currently studied to deliver the cells regardless of their source. Injection of dissociated RPE into the subretinal space showed photoreceptor rescue; however, this elegant minimally-invasive maneuver may not allow reformation of a polarized monolayer with the grafted cells.[8,9] The other strategy uses tissue engineering methods to grow the RPE on a scaffold mimicking Bruch's membrane (BM) to facilitate implantation and eventual integration in the subretinal space.[10] Transplanting a differentiated and polarized monolayer in the correct orientation could improve functionality and long-term survival of the RPE transplant.[11,12] However, placing an RPE monolayer transplant "on

Table 1. Results of Scraping According to Loop Material

Loop Material	Total Number of Blebs	HE Stained Probes	TB Stained Probes	Number of Blebs with Entirely Removed RPE*	Number of Blebs with Full-Thickness BM/CC Rupture*
PP 0.1 mm	23	13	10	23 (100%)	3 (13%)
PP 0.06 mm	4	2	2	3 (75%)	3 (75%)
Metal 0.1 mm	2	2	0	2 (100%)	2 (100%)
Controls	11	6	5		

* In relation to all scraped areas (HE and TB stained).

top" of the degenerated host RPE monolayer may trigger aberrant or unwanted cell signaling events. Furthermore, the remaining RPE under the graft may pose a mechanical barrier between transplanted cell patch and nutrition from the choriocapillaris (CC).

Candidate patients for RPE transplantations could differ in their stage of RPE degeneration. Patients with intermediate AMD or foveal sparing geographic atrophy (still) have an intact RPE monolayer. A still present, degenerating RPE leads to dysfunction in the neurosensory retina and its surrounding extracellular matrix (ECM). Hence, we hypothesize that, irrespective of any cause for RPE degeneration, cell source, or kind of transplantation mode that will turn out to be therapeutically successful, an atraumatic removal of host RPE within the targeted transplantation area may improve the success of RPE replacement strategies in animal models as well as candidate patient populations. Several techniques have been proposed to date for localized RPE removal and included subretinal scraping with custom instruments with or without ethylenediaminetetraacetic acid (EDTA) pretreatment,[13–15] fluid jet stream-assisted dislodging[13] or laser irradiation.[16,17]

We described a low cost surgical method for localized and atraumatic removal of the RPE which uses an extensible loop instrument. We tested three different loop materials to debride RPE in our previously described rabbit surgical model.[18] In an effort to reduce photoreceptor damage while manipulating beneath the bRD, we injected a cohesive viscoelastic into the subretinal space for stabilization. The immediate consequences of this subretinal maneuver then were analyzed by light and transmission electron microscopy (TEM).

Materials and Methods

Animals

We purchased 27 female and male chinchilla bastard rabbits weighing 2 to 2.5 kg from Charles River Laboratories (Sulzfeld, Germany). All procedures were approved by the state regulatory authorities of North Rhine-Westphalia (LANUV 8.87-50.1036.09.076 and 84-02.04.2014.A082) and in accordance with the ARVO Statement for the Use of Animals in Ophthalmic and Vision Research. Animals were held indoors in a specialized facility in an air-conditioned room with temperatures between 18°C and 20°C, exposure to regular daylight, in standardized individual cages with free access to food and water.

Instrumentation

The loop instrument consisted of a handpiece taken from a conventional, 15° angulated, 20 Gauge (G) vitreo-retinal instrument (Geuder AG, Heidelberg, Germany). It was combined with a 3.5-mm extensible loop within an oval nozzle at its distal, intraocular part (see Fig. 1). The loop was extended and retracted manually at its proximal, extraocular end to debride a targeted RPE surface. The respective loop designs differed in material and thickness: 0.06 vs. 0.1 mm polypropylene (PP; Prolene; Ethicon, Somerville, NJ) versus 0.1-mm metal wire (stainless chrome-nickel steel, DIN 17440; see Fig. 1; Tables 1, 2).

Surgery

The surgical technique was adapted from our previously published protocol.[18] In brief, pupils were dilated with 2.5% phenylephrine and 1% tropicamide eye drops, and rabbits were anesthetized by intramuscular injection of 65 mg/kg ketamine and 5 mg/kg xylazine or medetomidine 5 mg/kg. To better visualize the ocular fundus, the corneal epithelium was scraped with a surgical blade (No. 15; Feather Safety Razor, Co., Ltd., Osaka, Japan). A two-port, 23 G core vitrectomy (Megatron 4 HPS; Geuder AG) was performed through a noncontact, wide-angle system (BIOM II; Oculus, Wetzlar, Germany) with a 25 G or 27 G chandelier illumination system (Xenotron 3;

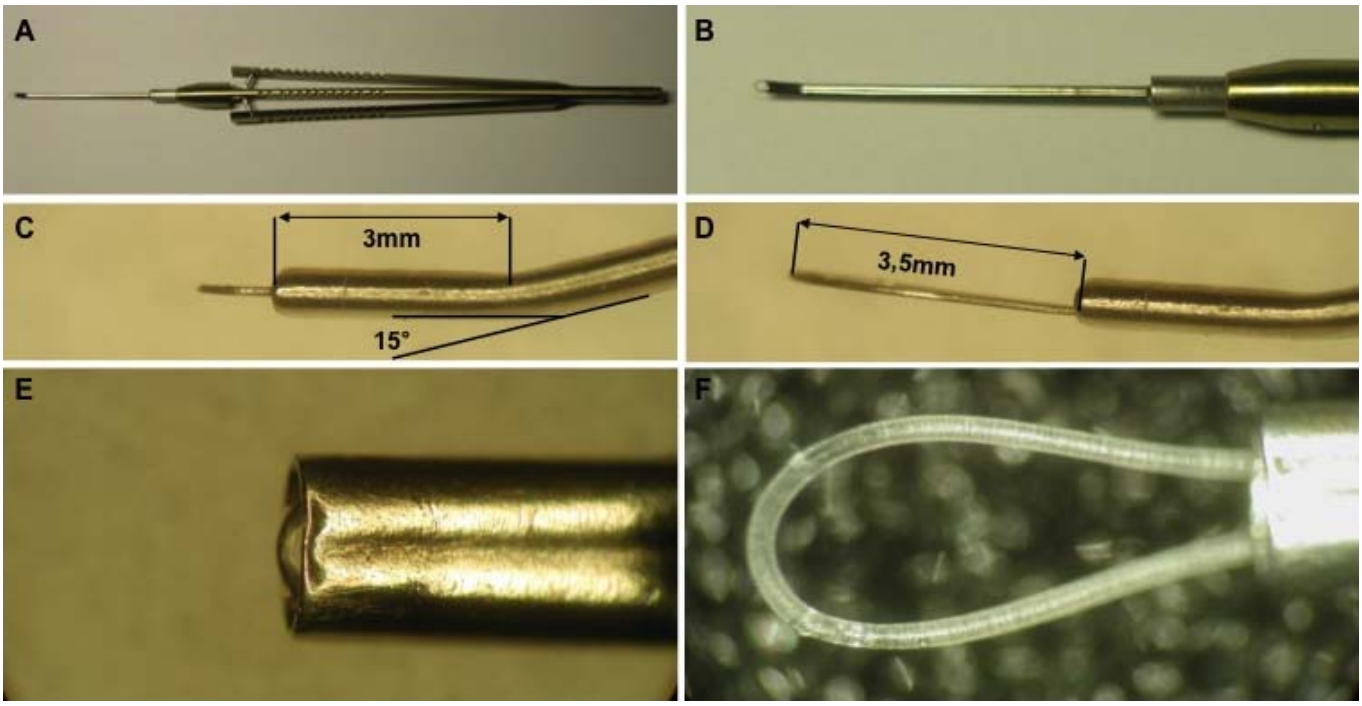

Figure 1. Loop instrument design. The overview on the RPE loop scraper shows a handpiece taken from conventional, 15° angulated, vitreoretinal instrument (A). In an enlargement on the functional distal instrument, part an oval metallic tube can be seen (B). In a side view the slightly extended loop within a 20 G oval nozzle at the distal, intraocular part of the instrument can be seen (C). The full extendable length of 3.5 mm can be seen in maximum extended position (D). (E) Top view of the distal intraocular part, with loop in retracted, primary position. (F) The loop is in the maximum extended position (top view).

Geuder AG; and Brightstar; D.O.R.C. Dutch Ophthalmic Research, Zuidland, The Netherlands, respectively). The posterior hyaloid face was engaged with the vitrectomy cutter in aspiration mode only, immediately inferior to the optic disc and then separated from the inner limiting membrane (ILM) using mechanical traction. The vitreous was then visualized with triamcinolone and thoroughly removed with the vitrectomy tip over the entire posterior pole.

Table 2. Overview of Surgical Variables

	Metal	PP 0.06	PP 0.1	Control Eyes with Surgery	Control Eyes without Surgery
No. of treated eyes	2	2	16	7	4
No. of blebs*	2	4	23		
Without HA	2	–	12		
HA 0.1	–	–	3		
HA 0.25	–	4	4		
HA 0.5	–	–	4		

* In some eyes 2 bRDs were raised concurrently.

Bleb retinal detachments (bRD) were raised by injection of balanced salt solution (BSS) (Puri Clear; Carl Zeiss Meditec AG, Jena, Germany) with an extendible 41 G subretinal injection needle (D.O.R.C. Dutch Ophthalmic Research) connected to a 100 µL Hamilton syringe (Hamilton syringe 710; Hamilton Bonaduz AG, Bonaduz, Switzerland) with the intraocular pressure (IOP) set to 25 mm Hg in a total of 27 eyes. The surgeon advanced the needle to the retinal surface and then an assistant slowly injected approximately 20 to 30 µL BSS to raise a bRD of approximately 3 disc diameters (DD). A retinotomy was performed by straight and/or vertically angled vitreoretinal scissors. The bRDs then were stabilized with various concentrations (0.1%, 0.25%, or 0.5%) of hyaluronic acid (HA; Gelbag; Carl Zeiss Meditec AG, molecular weight 2,500 kDa, sodium hyaluronate 1%), or BSS alone by injection with an 33-gauge cannula. For the respective concentrations noted above, the HA was diluted with sterile BSS, frozen for 30 minutes, warmed up to room temperature, and stirred. The RPE underneath the bRD was scraped at

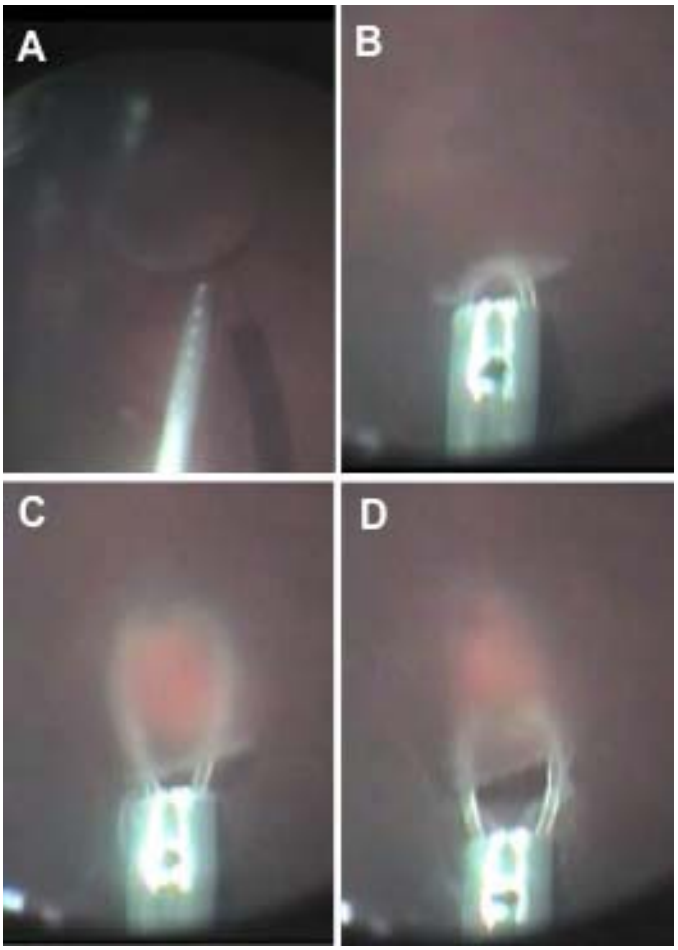

Figure 2. Surgical concept of RPE removal by the loop instrument. A bleb retinal detachment is created with a 41 G (Teflon) cannula (A). The loop instrument entering the subretinal space (B). Maximal extension in subretinal space apposed to BM with partially removed RPE (C). Afterwards, the loop is retracted over BM thereby completing the RPE wound (D).

high IOP (50 mm Hg), with 3 prototypes of a custom-made instrument (Geuder AG) in a total of 20 eyes (see Figs. 1–3), 7 eyes with bRDs alone served as controls. In some eyes ($N = 11$) two blebs were raised for scraping (Table 2). Sclerotomies and conjunctiva were sutured with 7-0 Vicryl (Ethicon) to ensure appropriate IOP and retinal adhesion for subsequent perfusion fixation.

Histologic Processing

The animals were euthanized with T61 in deep anesthesia immediately following the above surgical maneuver while the heads were fixed via carotid-perfusion with 2% glutaraldehyde (GA) or 4% paraformaldehyde (PFA). The eyes were enucleated immediately thereafter and immersed in the same fixative overnight. After removal of the anterior segments, the eyecups were photographed under a binocular microscope (Zeiss OPMI 1; Carl Zeiss Meditec AG) with a 5 megapixel smartphone digital camera (iPhone 4; Apple Inc., Cupertino, CA). Full thickness specimen (sclera, choroid, and retina) then were taken from the scraped bleb areas ($N = 29$), from normal control regions in eyes that underwent surgery ($N = 7$), as well as from control eyes ($N = 4$) without vitrectomy that served as controls (Table 2). The probes then were subjected to standard histologic processing. Embedded in paraffin ($N = 25$), 5-µm thick sections were cut with a microtome (Microm HM335E; MICROM International GmbH, Walldorf, Germany) and stained with hematoxylin and eosin (H&E). Embedded in Spurr's-resin ($N = 15$), semithin sections were cut at 1 to 2 µm on a ultramicrotome ("E"; Reichert, Leica Microsystems, Wetzlar, Germany) using a diamond knife (Ultra 45°; Diatome, Hatfield, PA), and stained with toluidine blue (TB). Some material was serially sectioned ($N = 21$), yet other material was only cut until a region of interest was encountered, for instance until blood clots ($N = 19$). Paraffin slides were stained by H&E, resin sections were stained by TB.

Evaluation of Histologic Probes

Serial sections were evaluated by light microscopy (Olympus BX50; Olympus, Shinjuku, Tokio, Japan) by two blinded observers (FT and MH) at different time points, assessing the quality of RPE debridement, lacerations in BM/CC and hemorrhages, and the integrity of the outer retina whenever preserved ($N = 15$). Full discontinuity in BM was considered as ruptured BM. Neurosensory layers within the bRD were assessed according to their continuity and integrity apart from minor damages to the outer retina.

Transmission Electron Microscopy

Ultrathin, 50-nm thick sections were taken from samples after RPE debridement with the 0.1 mm PP loop ($N = 7$) and bRDs alone ($N = 3$). They were contrasted with uranyl acetate and lead citrate thereafter.

The entire lengths of the ultrathin sections were analyzed using a Philips CM 10 transmission electron microscope (Philips, Eindhoven, The Netherlands). Ten sections per sample were cut. Images were taken with a Megaview 3 CCD digital camera and coupled with digital image software analysis (Olympus).

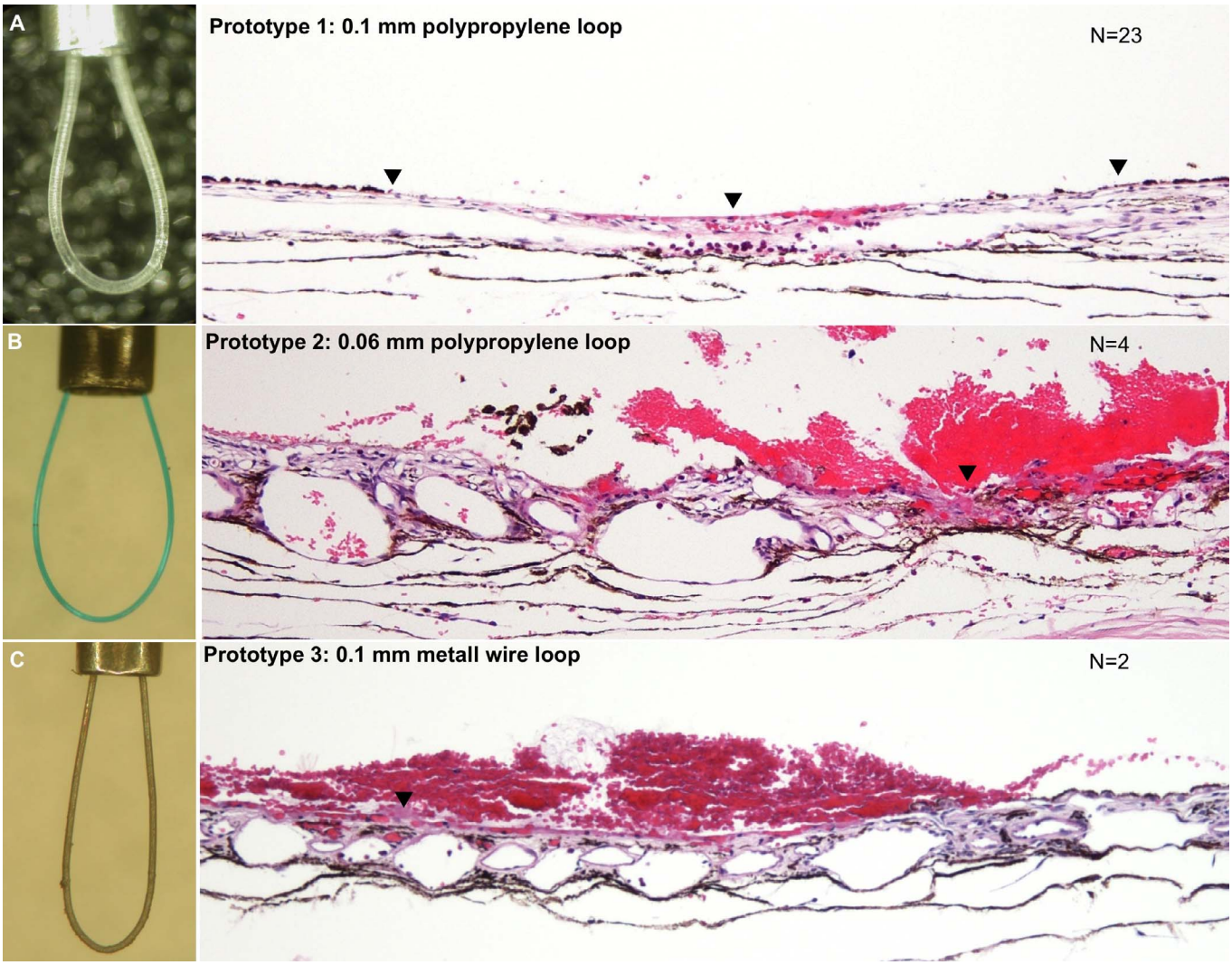

Figure 3. Characterization of prototype variants. Prototype 1, 0.1-mm PP loop, showed few BM defects, but nearly entirely RPE debrided areas. *Arrowheads* indicate RPE removed areas (A). Prototype 2, 0.06-mm PP loop, the less rigid material, showed insufficient debridement and extensive hemorrhages after multiple scraping maneuvers. *Arrowhead* indicates BM rupture (B). Prototype 3, 0.1-mm metal loop, showed multiple BM and CC ruptures and extensive subretinal hemorrhages in both operated eyes. *Arrowheads* indicate BM ruptures (C). *N* refers to number of scraping sites.

Results

Intraoperative Handling of Loop Scraper Instrument Prototypes

A localized retinal detachment was achieved by injection of BSS into the subretinal space in all animals (Supplementary Video S1). Injection of ≥0.25% HA into bRDs prevented neural retinal movements of the bRD during subretinal maneuvering with the loop scraper (Supplementary Videos S2). Blebs filled with 0.1% HA or BSS alone had a tendency to collapse upon manipulation (Supplementary Video S3).

To seek optimal material characteristics, we initially tested 3 different loop variants. Retinal pigment epithelium removal was possible with all loop material variants. Distinct transitions from pigmented to pale areas (= bare BM) were seen in every specimen subjected to scraping procedure (Figs. 2, 4).

The 0.1-mm thick PP loop yielded smooth and continuous sliding over the targeted RPE by 3 surgeons (BVS, SS, WW). After a single forward/backward stroke, an area of approximately 2.5 × 1.5

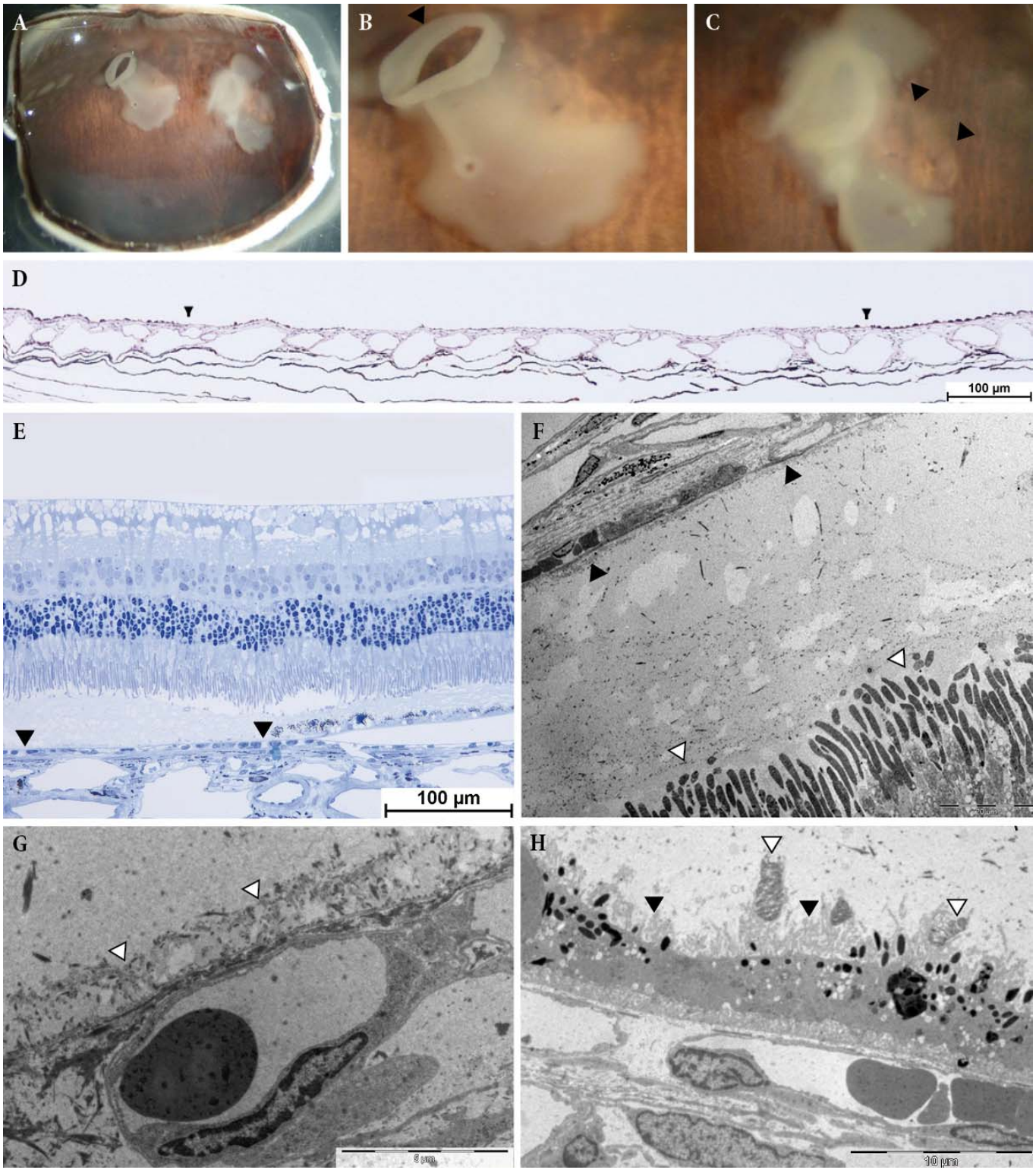

Figure 4. Representative morphology after RPE debridement (PP 0.1 mm). View on eyecup preparation with 2 bRD after perfusion fixation with GA (A). *Arrowhead* shows the retinotomy of the left bRD (B). Under the detached retina a pale, RPE debrided zone can be noticed (*arrowheads*) (C). A PFA-fixed section shows an RPE wound with distinct borders (*arrowheads*) (D). Choroid and neural retina adjacent to the RPE debridement seem to be of well-preserved morphology (*arrowheads* indicate the RPE debrided zone; [E]). In the absence of RPE, an integer choroidal vasculature, an intact BM (*black arrowheads*) and torn out, but preserved PR (*white arrowheads*) in

→

←
the detached retina can be noticed in TEM (F). Some plicated structures reminiscent of basolateral RPE infoldings (*white arrowheads*) overlying BM and choriocapillaris vessels could be seen in TEM (G). The RPE surface over nondebrided areas showed regular microvilli content (*black arrowheads*) along with some torn out bits of POS structures (*white arrowheads*) (H). *Scale bar*: in *lower right* of each micrograph indicates respective magnification.

mm (measured on flat mount preparation) was devoid of RPE as per view from the surgical microscope (Supplementary Video S1). Blanching of choroidal vasculature was observed particularly on the backstroke. No retinal adhesion to instrument parts during and no subretinal bleeding after the maneuver in the subretinal space were observed. Some RPE clumps were typically adherent to the loop, their remains were removed successfully with the vitrectomy tip or soft tip flute needle.

The 0.06-mm thick PP loop seemed too elastic when apposed to the RPE surface, compared to the 0.1-mm PP loop. Removal of the RPE seemed incomplete with a single forward/backward loop movement over the targeted area, 2 to 3 strokes over the same area then appeared to remove the pigmentation. No subretinal hemorrhage had been observed intraoperatively.

The 0.1-mm metal wire loop "got trapped" after apposition to the RPE surface and some further extension under the bRD, to then immediately thereafter reveal an extensive subretinal hemorrhage, despite the IOP settings at 50 mm Hg on the vitrectomy machine.

Given the consistent desirable results on localized RPE debridement with the 0.1-mm PP loop, further detailed evaluation then was limited to this instrument prototype.

Histologic Evaluation of RPE Removal

Effect on BM/CC Complex

The BM/CC complex and its integrity could be better characterized when evaluating HE stained specimens (Table 1). Therefore, we concentrated on the HE-stained samples from scraped areas ($N = 25$), yet counted any ruptures and hemorrhages in TB-stained samples ($N = 15$). Using PP 0.1 mm for a single forward/backward stroke, almost entirely debrided areas of RPE were observed macroscopically and histologically (Figs. 3A, 4, 5). The BM was split and thinned in most cases of scraped areas in HE-stained slices ($N = 10$). Apart from very few full thickness lacerations in BM and correlating CC blood clots ($N = 2$), BM layers were continuous. Histology of the 0.1-mm PP loop obtained from the edge of the RPE wound showed distinct, sharp transitions from pigmented to bare areas. Choroidal vasculature appeared intact (Figs. 4D, 4F, 4G). However, few extravascular clots of erythrocytes and corresponding BM ruptures could be seen (Fig. 5).

A single scrape with PP 0.06 mm, the less rigid material, resulted in unsatisfactory RPE debridement,

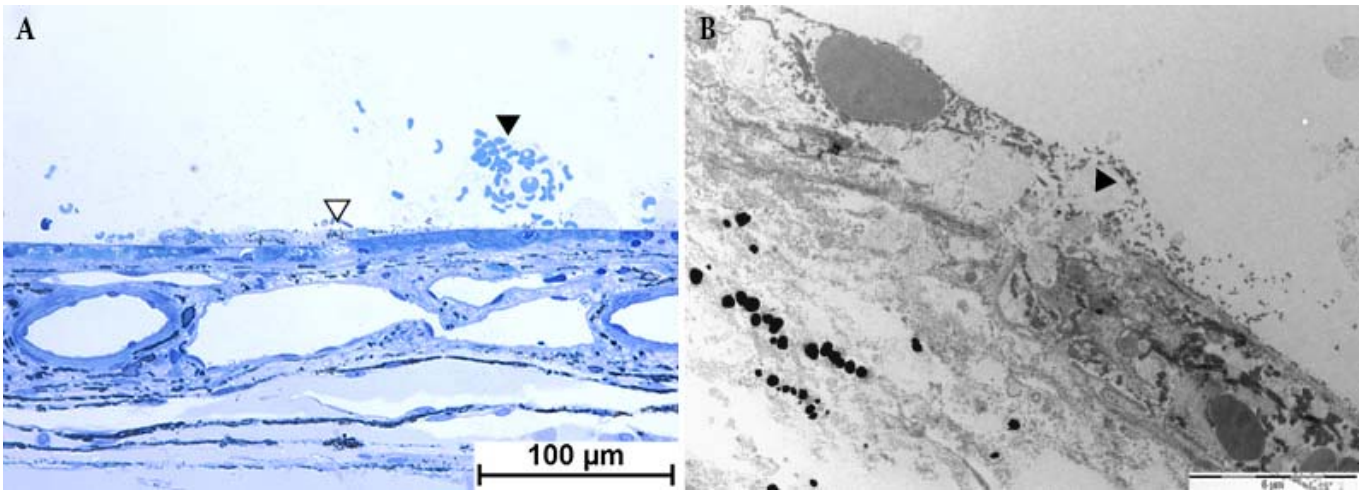

Figure 5. Evidence for traumatic lesions within RPE-scraped area (with PP 0.1 mm). Extravascular erythrocytes (*black arrowhead*) indicate BM/CC ruptures. The *white arrowhead* shows a small BM lesion (A). Details of a BM lesion can be seen at higher magnification by TEM. Bruch's membrane is ruptured in its full thickness (*arrowhead*; [B]).

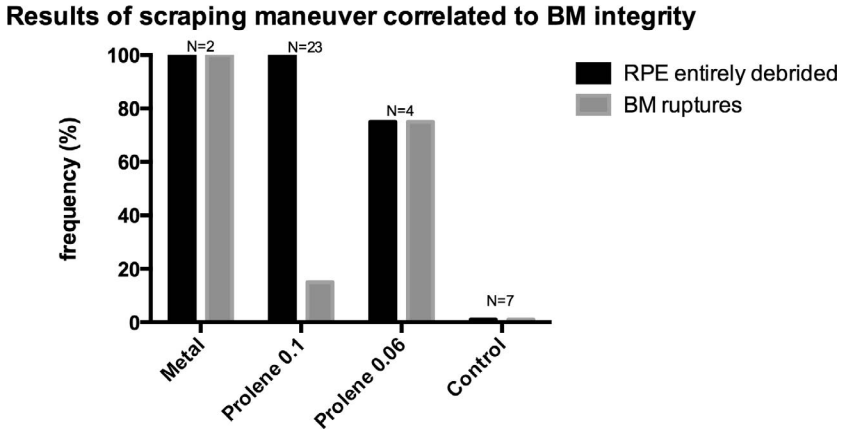

Figure 6. Results of scraping correlated to BM integrity. Bruch's membrane ruptures and RPE debrided areas were summarized and correlated to the material of the loop instrument. *N* refers to the numbers of scraping areas.

while repeated scraping maneuvers caused more BM defects and extensive hemorrhages compared to the 0.1-mm PP loop (Figs. 3B, 6; Table 1). Retinal pigment epithelium debridement with the most rigid material, the 0.1-mm thick metal loop, resulted in massive intraoperative subretinal hemorrhages (Fig. 3C).

To further evaluate the effects of the scraping maneuver with the 0.1-mm PP loop on the integrity of BM/CC complex we performed TEM. The debrided areas were free of intact RPE cells albeit leaving some residual pigment and plicated structures reminiscent of basolateral RPE infoldings behind (Fig. 4G). Rarely, ruptures of BM could be identified on TEM. Erythrocytes overlying BM suggested its rupture (Fig. 5).

Controls of operated eyes with bRD alone and control sections of eyes without any surgery showed normal histology suggesting that intraoperative high IOP did not cause BM/CC ruptures and/or choroidal hemorrhages (data not shown). In peripheral areas with intact RPE and adherent retina, well-preserved microvilli incorporating photoreceptor outer segments (POS) were seen on TEM (data not shown).

Effects on Neural Retina

Retina was part of the embedded tissue only in some cases ($N = 13$). Due to this fact, we did not quantify and correlate morphology of the retina to the loop material used. Using $\geq$0.25% HA, retinal layers were continuous, without signs of thinning or tearing in the area overlaying the debrided zone. The POS integrity appeared to be maintained without any apical RPE residues throughout the bRD (Figs. 4E, 4F). On TEM, however, occasional short bits of torn out POS were observed still invaginating into RPE microvilli, suggesting minor trauma to the outer retina (Fig. 4H).

Discussion

An elastic loop scraper instrument can effectively remove the RPE during vitrectomy and largely preserve the underlying BM and choriocapillaris. This technique might be helpful to precede RPE transplantation in cases of degenerated host RPE. The loop concept minimizes actual instrument "volume." A smooth material surface enables even sliding with minimal chance for tissue laceration. Loop elasticity and curvature avoid traumatic rupture by compensating too harsh movements by the surgeon. The pressure applied by each surgeon however, cannot be standardized. Instrument design with the loop concept and choice likely make the differences among surgeons negligible. Nevertheless, despite geometric constraints imposed by ocular anatomy, wound construction and actual instrument angulation the surgeon might, in theory, have forced more or less power in a vertical vector to the choroid (probable causing hemorrhage). However, the crucial vector to debride the RPE is tangential to the RPE and could not be influenced by different pressure.

The degree of elasticity of loop materials, however, also determined the extent of choroidal trauma and efficacy of RPE debridement. The highly rigid metal loop caused BM/CC lacerations with macroscopic hemorrhage. Surprisingly, using elastic 0.06-mm PP loops resulted in insufficient RPE removal, while multiple scraping maneuvers caused bleedings. Surgery with an elastic, but still sufficient rigid material, 0.1-mm PP, resulted in satisfactory removal of RPE

with minimal trauma in rabbits. Preliminary experiments with subretinal surgery in anesthetized pigs could confirm surgical handling and histologic characteristics of the 0.1-mm PP loop device.

The present study is limited to acute data obtained during the described surgical maneuver. We caution against any interpretation of possible long-term consequences of the RPE scraping and/or subretinal viscoelastics on the retina; these experiments will be the subject of future work.

Existing technologies for RPE debridement, such as hydraulic debridement suggested by Lane[19] or Leonard,[13] may cause dispersion of the RPE into the vitreous, thereby stimulating proliferative vitreoretinopathy. Moreover, the denuded area was variable in size, and associated with macroscopic[13] and microscopic[19] hemorrhages, fibrin, and flattened capillaries. Leonard[13] observed cellular damage of the neural retina with intracellular edema. Moreover, compared to our loop approach, these existing technologies require longer subretinal manipulation while possibly being less efficient at RPE removal and combined with the forceful and repeated jet stream may be more likely to cause photoreceptor damage. Abrasive debridement with a silicone soft tip[13] or metal tip[14,20] can induce breaks and damages to the BM/CC complex through less controlled and direct transmission of vectorial forces exerted by the surgeon's hand on the instrument. Ethylediaminetetraacetic acid–facilitated removal of the RPE[15] will open tight junctions of the RPE, thereby loosening cell–cell adhesion, but rather not cell–substrate adhesion, yet may ease eventual mechanical RPE removal. Ethylediaminetetraacetic acid has documented photoreceptor toxicity, however,[21] and, therefore, is unlikely to be used in patients. Attempts for exclusive RPE destruction by laser present to date with unique and costly challenges, but seem feasible with pulsed laser technology without collateral damage to BM or PR.[22,23]

Irrespective of loop material, reflux from the BSS-filled bRD induced by the loop instrument led to partial collapse of the bRD and hindered subretinal manipulation. The effect was comparable to a passive flute needle effect; technical constraints in instrument design limited complete elimination of this phenomenon. To stabilize the bRD, we injected a cohesive ocular viscoelastic device (OVD) of $\geq$0.25% in BSS. The stabilizing cohesive effects[24] successfully prevented accidental retinal damage during maneuvering with the loop scraper. Cohesive OVD are space-fillers and by definition will not adhere to tissue as opposed to dispersive gels. Thus, it will feel easy for the surgeon to get the OVD out of the SRS, for example, by an extrusion instrument with a brushed silicone tip.

Tiny ruptures in BM and CC, as observed with the PP 0.1-mm loop, might be negligible in the case of carrier-supported RPE monolayer transplantations. However, RPE suspensions exposed to deeper layers of BM created by abrasive surgical maneuvers similar to our loop instruments have higher rates of apoptosis,[25] or tend not to reattach and have lower proliferation rates.[25,26] However, we did not analyze the extent of a possible BM basal laminar damage, and, therefore can only speculate on this effect.

Our loop instrument could help in other cases of microsurgical debridements in ophthalmic surgery, for example anterior and posterior lens capsule polishing as well as the peeling of epiretinal membranes. Removal of residual lens epithelial cells might prevent anterior capsule contraction and posterior capsular opacification (PCO), a common complication of cataract surgery.[27,28] Epiretinal membranes might be lifted at a broader base with less force and consequently reduced collateral damage.

Finally, this work might help to develop an animal model with limited resemblance to macular degenerations with geographic atrophy by imitating the loss of RPE, along with its associated secondary consequences causing CC and photoreceptor atrophy. Surgical removal of a choroidal neovascularization/CNV (a former indication for RPE transplantation), or an acute RPE rip, such as it occurs occasionally during anti-VEGF therapy for exudative AMD, in pigment epithelial detachments with associated or suspected CNV (an inclusion criterion in the London Project to cure blindness) probably would represent a quite similar condition to our pilot data presented here.

Taken together, we have developed a prototype instrument design for selective RPE debridement in a rabbit model. These data are an encouraging foundation for future studies on biointegration of cell carrier-based RPE transplantation through tissue engineering.

Acknowledgments

This study was presented in parts at the 4th TERMIS World Congress 2013 "Tissue Engineering and Regenerative Medicine," Istanbul, Turkey, June 17–20, 2013; at the 111th DOG Congress 2013

"Deutsche Ophthalmologische Gesellschaft," Berlin, Germany, September 19–22, 2013; at the annual meeting of the Association for Research in Vision and Ophthalmology (ARVO), Orlando, Florida, USA, 2014; and at the 112th DOG Congress 2014 "Deutsche Ophthalmologische Gesellschaft," Leipzig, Germany, September 25–28, 2014.

The authors thank Claudine Strack for her technical assistance in the laboratory.

Supported by Rüdiger Foundation grants (BVS), BONFOR/Gerok Scholarship O-137.0015 (BVS), BONFOR/Gerok Scholarship O-137.0019 (FT), and by Deutsche Forschungsgemeinschaft/DFG (BVS) STA 1135/2-1. Some research materials were provided by Geuder AG at no cost.

Disclosure: **F. Thieltges**, None; **Z. Liu**, None; **R. Brinken**, European patent application PCT DE/2013/200320; **N. Braun**, European patent application PCT DE/2013/200320; **W. Wongsawad**, None; **S. Somboonthanakij**, None; **M. Herwig**, None; **F.G. Holz**, European patent application PCT DE/2013/200320; **B.V. Stanzel**, European patent application PCT DE/2013/200320

References

1. Binder S, Stanzel BV, Krebs I, Glittenberg C. Transplantation of the RPE in AMD. *Prog Retin Eye Res*. 2007;26:516–554.
2. Buchholz DE, Hikita ST, Rowland TJ, et al. Derivation of functional retinal pigmented epithelium from induced pluripotent stem cells. *Stem Cells*. 2009;27:2427–2434.
3. Haruta M, Sasai Y, Kawasaki H, et al. In vitro and in vivo characterization of pigment epithelial cells differentiated from primate embryonic stem cells. *Invest Ophthalmol Vis Sci*. 2004;45:1020–1025.
4. Gouras P, Flood MT, Kjeldbye H. Transplantation of cultured human retinal cells to monkey retina. *An Acad Bras Cienc*. 1984;56:431–443.
5. Enzmann V, Howard RM, Yamauchi Y, Whittemore SR, Kaplan HJ. Enhanced induction of RPE lineage markers in pluripotent neural stem cells engrafted into the adult rat subretinal space. *Invest Ophthalmol Vis Sci*. 2003;44:5417–5422.
6. Vossmerbaeumer U, Ohnesorge S, Kuehl S, et al. Retinal pigment epithelial phenotype induced in human adipose tissue-derived mesenchymal stromal cells. *Cytotherapy*. 2009;11:177–188.
7. da Cruz L, Chen FK, Ahmado A, Greenwood J, Coffey P. RPE transplantation and its role in retinal disease. *Prog Retin Eye Res*. 2007;26:598–635.
8. Carr AJ, Vugler AA, Hikita ST, et al. Protective effects of human iPS-derived retinal pigment epithelium cell transplantation in the retinal dystrophic rat. *PLoS One*. 2009;4:e8152.
9. Lund RD, Wang S, Klimanskaya I, et al. Human embryonic stem cell-derived cells rescue visual function in dystrophic RCS rats. *Cloning Stem Cells*. 2006;8:189–199.
10. Lu B, Tai YC, Humayun MS. Microdevice-based cell therapy for age-related macular degeneration. *Develop Ophthalmol*. 2014;53:155–166.
11. Diniz B, Thomas P, Thomas B, et al. Subretinal implantation of retinal pigment epithelial cells derived from human embryonic stem cells: improved survival when implanted as a monolayer. *Invest Ophthalmol Vis Sci*. 2013;54:5087–5096.
12. Stanzel BV, Liu Z, Somboonthanakij S, et al. Human RPE stem cells grown into polarized RPE monolayers on a polyester matrix are maintained after grafting into rabbit subretinal space. *Stem Cell Rep*. 2014;2:64–77.
13. Leonard DS, Zhang XG, Panozzo G, Sugino IK, Zarbin MA. Clinicopathologic correlation of localized retinal pigment epithelium debridement. *Invest Ophthalmol Vis Sci*. 1997;38:1094–1109.
14. Phillips SJ, Sadda SR, Tso MO, Humayan MS, de Juan E Jr, Binder S. Autologous transplantation of retinal pigment epithelium after mechanical debridement of Bruch's membrane. *Curr Eye Res*. 2003;26:81–88.
15. Del Priore LV, Hornbeck R, Kaplan HJ, et al. Debridement of the pig retinal pigment epithelium in vivo. *Arch Ophthalmol*. 1995;113:939–944.
16. Quiroz-Mercado H, Yeshurun I, Sanchez-Buefil E, Guerrero-Naranjo JL, Luloh P, Mercellino GR. Subretinal, viscoelastic-assisted, endoscope-guided photothermal ablation of choroidal neovascular membranes by Erbium:YAG laser. *Ophthal Surg Lasers*. 2001;32:456–463.
17. Jobling AI, Guymer RH, Vessey KA, et al. Nanosecond laser therapy reverses pathologic and molecular changes in age-related macular degeneration without retinal damage. *FASEB J*. 2015;29:696–710.
18. Stanzel BV, Liu Z, Brinken R, Braun N, Holz FG, Eter N. Subretinal delivery of ultrathin rigid-elastic cell carriers using a metallic shooter

instrument and biodegradable hydrogel encapsulation. *Invest Ophthalmol Vis Sci*. 2012;53:490–500.
19. Lane C, Boulton M, Marshall J. Transplantation of retinal pigment epithelium using a pars plana approach. *Eye*. 1989;3:27–32.
20. Rabenlehner D, Stanzel BV, Krebs I, Binder S, Goll A. Reduction of iatrogenic RPE lesions in AMD patients: evidence for wound healing? *Graefes Arch Clin Exp Ophthalmol*. 2008;246:345–352.
21. Szurman P, Roters S, Grisanti S, et al. Ultrastructural changes after artificial retinal detachment with modified retinal adhesion. *Invest Ophthalmol Vis Sci*. 2006;47:4983–4989.
22. Wood JP, Shibeeb O, Plunkett M, Casson RJ, Chidlow G. Retinal damage profiles and neuronal effects of laser treatment: comparison of a conventional photocoagulator and a novel 3-nanosecond pulse laser. *Invest Ophthalmol Vis Sci*. 2013;54:2305–2318.
23. Lorach H, Kung J, Beier C, et al. Development of animal models of local retinal degeneration. *Invest Ophthalmol Vis Sci*. 2015;56:4644–4652.
24. Rouse PE. A theory of the linear viscoelastic properties of dilute solutions of coiling polymers. *J Chem Phys*. 1953;21:1272–1280.
25. Tezel TH, Kaplan HJ, Del Priore LV. Fate of human retinal pigment epithelial cells seeded onto layers of human Bruch's membrane. *Invest Ophthalmol Vis Sci*. 1999;40:467–476.
26. Gullapalli VK, Sugino IK, Van Patten Y, Shah S, Zarbin MA. Impaired RPE survival on aged submacular human Bruch's membrane. *Exp Eye Res*. 2005;80:235–248.
27. Awasthi N, Guo S, Wagner BJ. Posterior capsular opacification: a problem reduced but not yet eradicated. *Arch Ophthalmol*. 2009;127:555–562.
28. Steinberg EP, Javitt JC, Sharkey PD, et al. The content and cost of cataract surgery. *Arch Ophthalmol*. 1993;111:1041–1049.